

Studying of sintered WC-8Co powder with coatings of aluminum oxide produced by atomic layer deposition

Maxim Yu Maximov*, Aleksandr S Verevkin, Anna A Orlova, Pavel A Novikov, Aleksey O Silin, Oleg V Panchenko and Anatoly A Popovich

Peter the Great Saint-Petersburg Polytechnic University, 195251, St. Petersburg, Russia

Grain size reduction in cemented carbides leads to higher mechanical properties. Therefore, preventing the grain growth during sintering is a crucial task. This study proposes the application of Al₂O₃ coatings obtained by atomic layer deposition (ALD) on WC-8Co powder, where Al₂O₃ is added as a grain growth inhibitor. After deposition, the films were found both on separate particles and on the dense agglomerates. The thickness of aluminum oxide varied in the range of 30-100 nm depending on the synthesis parameters and the powder's bulk density. Composite particles were compacted using spark plasma sintering (SPS). The compacted samples density was about 99-99.6% of the theoretical. Alumina was found on the grain boundaries of tungsten carbide.

Key words: Cemented carbides, WC-8Co, Atomic layer deposition, Aluminum oxide, Grain growth inhibitor, Spark plasma sintering.

Introduction

Advanced cermet materials based on tungsten carbide and cobalt have been widely used for tools production and in tribology due to their combination of such important properties as high hardness, wear, and fracture resistance [1]. For example, WC-Co alloys have high strength and hardness because of its composition and structure, and hard carbide is permeated with a soft and ductile cobalt binder.

High-hardness compact unstructured cermet materials based on tungsten carbide and cobalt are difficult to obtain due to rapid grain growth during sintering, which causes to low mechanical properties and adversely affected on quality of final products. Conventional sintering technology includes heating of the compacts up to 1400-1500 °C. At this temperature, liquid eutectic is formed and significant grain growth occurs through the liquid phase [1]. Spark plasma sintering is a quick and reliable way of obtaining compact samples. Pulsed high power DC current which passes through the sample in the SPS process achieves high heating rates (up to 1000 °C/min) and applied pressure activates the mass transfer at a relatively low temperature (0.5-0.9 T_m). Rapid heating and short isothermal holding time at a relatively low temperature prevents intense grain growth [2]. The electroplastic effect in the sample under the influence of the high intensity electromagnetic field occurs and enhances mass transfer in the solid phase

[3]. Spark plasma sintering of WC-Co-based cermet is performed at a wide range of temperatures (from 900 to 1280 °C) and pressures (from 25 to 100 MPa) with isothermal holding time from 5 to 30 minutes. Using such parameters, minimal porosity can be achieved (about 0.01%) [4-6].

To prevent the grain growth of the carbide phase, the most effective way is the use of growth inhibitors such as metals carbides and oxides [2]. It is advisable to use, as inhibitor, the materials that do not disrupt the structure of the cemented carbide, do not melt, and do not form compounds and solid solutions with cobalt and tungsten carbide at the sintering temperature. Furthermore, the structure of cemented carbide should not be agglomerations, which cause stress concentration. One of such materials is Al₂O₃ [7]. Aluminum oxide has high heat-resistance, wear-resistance, chemical resistance, and low friction coefficient [1, 8]. There are some studies that describe the creation of a cermet composite based on tungsten carbide and aluminum oxide powders with metal binders [9-13]. Deposition of coatings directly on the tungsten carbide powder with further sintering is a new approach to obtain cermet compact materials.

Deposition of alumina film on powders is one of the methods to obtain complex composites with a uniformly distributed inhibitor. Atomic layer deposition (ALD) is one of the methods of thin film production, and its basic principles are based on self-controlled reactions at the monolayer level with the functional groups of the matrix surface [14, 15]. This method allows the deposition of films with varying thickness and precision accuracy both on flat-surface substrates and on powder materials and it can provide high adhesion coatings due to

*Corresponding author:
Tel : +7 (931) 004-17-23
Fax: +7 (812) 294-46-20
E-mail: maximpsbstu@mail.ru

chemical interaction with the substrate surface. ALD is widely used to obtain thin films of oxides, including aluminum oxide.

Methodology

The initial commercially available WC-8Co powder (SC Kirovgrad Hard Alloys Plant, 99%) was used for the deposition of thin films of aluminum oxide and further sintering.

Trimethylaluminium (TMA- $\text{Al}(\text{CH}_3)_3$, CAS #75-24-1, 99.999%, Russia) and deionized water was used as precursors for Al_2O_3 coatings by atomic layer deposition (ALD).

The phase composition and morphology of the initial WC-8Co powder were studied by X-ray diffraction (XRD, Bruker D8 Advanced, $\text{CuK}\alpha$ $\lambda = 1.54059 \text{ \AA}$, scanning step of 0.02° (2θ scale), exposure time of 10 s, in the 2θ range from 30° to 80°) and scanning electron microscopy (Mira 3 Tescan, Oxford X-max^N EDX, 20 kV) at SPbPU. To determine the average crystallite size of the tungsten carbide particles, Rietveld refinement was performed using the TOPAS software package.

The particle size distributions were examined using a laser particle size analyzer (Laser Diffraction) Analysette 22 NanoTec plus (Fritsch). Deposition of aluminum oxide coatings on WC-8Co powders was performed on the atomic layer deposition (ALD) system Picosun R-150 equipped with a chamber for thin layer deposition on powder materials POCA-200 at the SPbPU Research Laboratory "Functional Materials." POCA-200 is special camera with micron diameter holes in the vertical direction for the passage of gas and reagents directly through powder. Synthesis temperature of 300°C was chosen based on the ALD temperature window and due to the high growth rate per cycle, more than 1 \AA/cycle according to [16]. The number of ALD cycles varied from 70 to 150. A single ALD cycle includes three consecutive supplies of TMA (pulse time - 0.1 s, blowing time between pulses - 1 s) with subsequent 60 s blowing and three consecutive supplies of H_2O (pulse time - 0.1 s, blowing time between pulses - 1 s) with subsequent 90 s of blowing. The temperature of precursor tanks was maintained at 25°C . About 20 g of powder was loaded into the POCA-200 chamber. Pressure during synthesis was about 17-20 hPa. The holding time of powder was set for 1 hr at the pressure and the synthesis temperature.

The morphology and thickness of the films obtained on WC-8Co powders surface were studied on the cross-beam SEM-FIB workstation Zeiss Auriga Laser. Cross-sections were made by a focused gallium ion beam with accelerating voltage of 30 kV and beam currents of 4 A, 600 A, and 50 A at the initial, intermediate, and final stages, respectively. The secondary electron signal was used to build images. The angle between the electron gun and the ion gun was 45 degrees. The investigations were made in the resource center "Nanotechnology" of

the Research Park, SPbSU.

The sintering of the WC-8Co powders before and after deposition of Al_2O_3 was carried out by spark plasma sintering (SPS) on the HP D 25 system (FCT Systeme GmbH - Spark Plasma Sintering Furnace type HP D 25, Germany). The average duration of the sintering process time was 40 min. The heating is performed by passing DC pulse current at the heating rate of $100^\circ\text{C}/\text{min}$. High temperature holding time was 30 minutes at 1300°C , ambient pressure less than 10^{-3} bar, and pressing force at sintering - 16 kN. Sintering was performed in a graphite mold with an inside diameter $\text{O}20 \text{ mm}$ at 2.5 g of powder, and graphite foil gaskets are used to protect the mold.

Sections of the sintered materials were embedded into resin and polished with diamond grinding disc ($54 \mu\text{m}$ grit) and diamond suspension (9 and $3 \mu\text{m}$) perpendicularly to the SPS pressing direction. Alumina free polishing was used to prevent contamination of polished section by abrasive of aluminum oxide. Macro hardness tests were conducted on a universal hardness tester ZHU 187.5 (Zwick Roell AG, Germany) using a load of 10 kg and a dwell time of 10 sec. The reported value was the average of at least 10 indentations.

Results and Discussion

The WC-8Co powder characterization was performed at the first research stage. The particle-size distribution and powder morphology of the initial material is shown in Fig. 1. Figure 1(a) shows frequency and cumulative distribution based on a volumetric assumption. The cumulative size distribution is $0.5 \mu\text{m}$, $1.8 \mu\text{m}$ and $4 \mu\text{m}$ for d_{10} , d_{50} and d_{90} , respectively. Powder particles size of the observed in the SEM micrographs (Fig. 1(b)) was in agreement with the results obtained by a laser analyzer. The initial powder material is a mechanical mixture of tungsten carbide and cobalt metal powders, where tungsten carbide consists of the WC phase and W_2C impurities. The tungsten carbide particles morphology is angular. Cobalt particles have a rounded shape.

Atomic layer deposition in a test mode (300°C -100 ALD cycles) checked the possibility of alumina oxide deposition onto WC-8Co powder. The chemical

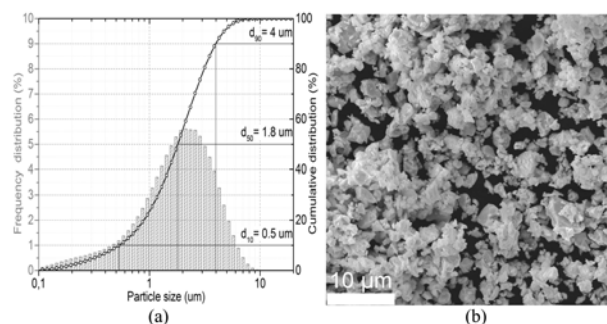


Fig. 1. (a) Particle-size distribution and (b) morphology of the WC-8Co initial powder.

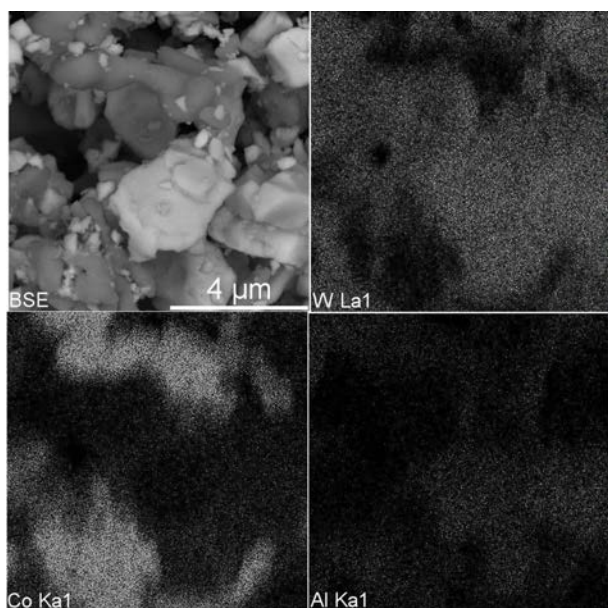


Fig. 2. SEM-EDX investigation of chemical distribution of the WC-8Co powder after alumina deposition. BSE image with the corresponding EDX elemental mapping results of WC-8Co with Al_2O_3 coatings.

composition of the obtained particles surface was determined by EDX mapping in a random powder probe (Fig. 2). Aluminum and oxygen were found over the entire surface of the material; thus, alumina is present both on cobalt and tungsten carbide particles.

To study the morphology, thickness, and integrity of the coatings, Al_2O_3 was synthesized at 300 °C during 70 and 150 ALD cycles onto WC-8Co powder. Cross-sections of the coated powder samples were made by

focused gallium ion beam and presented at Fig. 3.

Studying the coated samples obtained under different number of ALD cycles have shown similar results. The powder samples contained tungsten and cobalt particles separately. Almost all of the particles are covered by alumina partially or completely.

In the WC-8Co samples with aluminum oxide obtained during 150 cycles, average film thickness is about 30 nm. However, some particles have thicker coating up to 100 nm, probably due to uneven density of powder filling. We suppose that in the space with high density of powder filling the passage of gas with reagent is limited, which leads to the accumulation of the TMA, H_2O and formation of a thicker layer.

Fig. 3(a) and 3(b) demonstrate that the films are primarily formed on dense agglomerations. However, in locations of close contact between the particles, where the van der Waals interaction is possible, there are no coatings. Therefore, the uncoated surfaces and particles may be the result of particles fracturing during powder sample preparation. Agglomerated segments with coatings could be partly destroyed during powder mixing for making probe, and it leads to appearance of uncoated surfaces.

In the samples with Al_2O_3 obtained during 70 cycles, coatings are presented on the agglomerates, as in case of samples with films synthesized at 150 ALD cycles. Analysis of the results obtained using backscattered electrons (BSE) shows the presence of coatings on cobalt (dark particles) and tungsten carbide (light particles) (Fig. 3(c)).

For the particles with 70 ALD cycles, the films on the surface are significantly thinner 10-20 nm than in

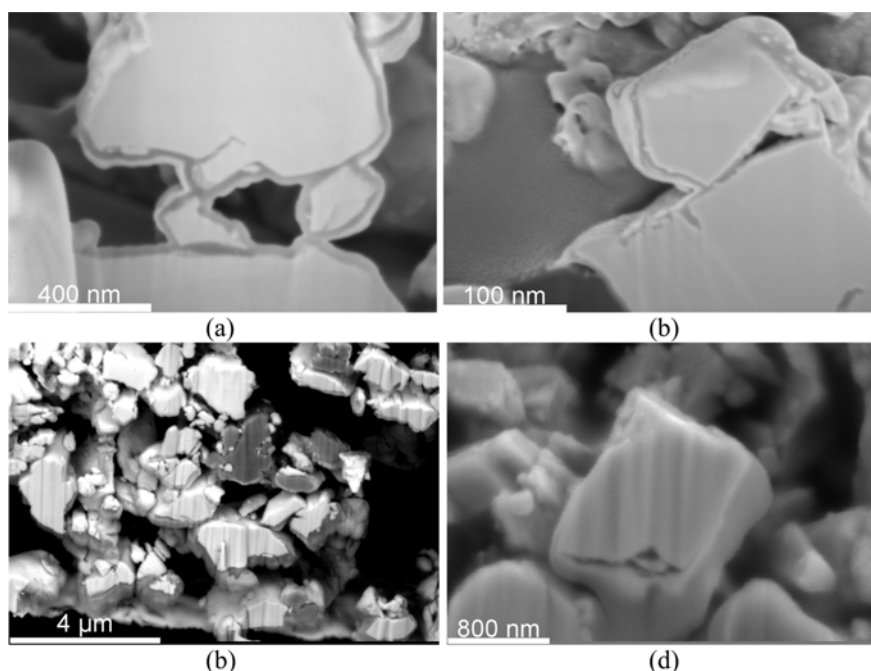


Fig. 3. Cross-sections of WC-8Co powder samples with alumina coatings. (a,b) 150 ALD cycles, (c,d) 70 ALD cycles.

case of 150 ALD cycles and during gallium ion cutting, and in some cases, it could be destroyed because of the high-energy beam. Therefore, the top surfaces of some particles have no alumina coating of (Figs. 3(c) and 3(d)). It could be also due to uneven density of initial powder filling. However, aluminum is visible in the spectra of energy-dispersive X-ray microanalysis (EDX), Fig. 2.

Powders with aluminum oxide and without were compacted by the SPS method.

XRD data shows (Fig. 4) that initial tungsten carbide powder has good crystallinity with diffraction peaks corresponding to the (001), (100), (101), (110), (002), (111), (200), (102) planes of hexagonal lattice structure with P-6m2 space group (ICDD No. 00-051-0939). The small amount of W_2C impurities were detected in initial powder. Planes of hexagonal lattice structure (110), (002), (-1-11), (-1-12), (300), (-1-13) (ICDD No. 01-079-0743) with P-31m space group were related to the W_2C phase. Cobalt phase can be found with (111) and (200) planes of FCC lattice structure with the Fm-3m space group (ICDD No. 00-015-0806) in the initial powder.

Sintered samples according to XRD patterns consist of WC phase. Alumina and W_2C phases were not detected. Furthermore, according to [11], the addition of small amount of aluminum oxide prevents the formation of W_2C during sintering. In addition, SPS method allowed the W_2C phase content to decrease in sintered samples.

XRD data shows that the diffraction peaks of all sintered samples are shifted to the lower angles compared to powder. This shift refers to lattice parameter growth induced by heating during spark plasma sintering. The sintered WC-8Co without Al_2O_3 coatings show maximum diffraction peaks shift. The lower peaks shift corresponds to the sintered sample with a thicker alumina coating (150 ALD cycles).

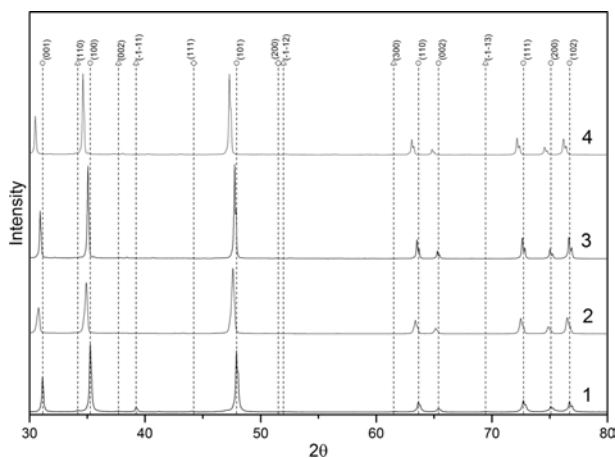


Fig. 4. XRD patterns obtained from WC-8Co powder and sintered WC-8Co with and without ALD treatment. (1) initial powder, (2) sintered after 70 ALD cycles, (3) sintered after 150 ALD cycles; (2) sintered powder; (○) WC, (◇) W_2C , (△) - Co.

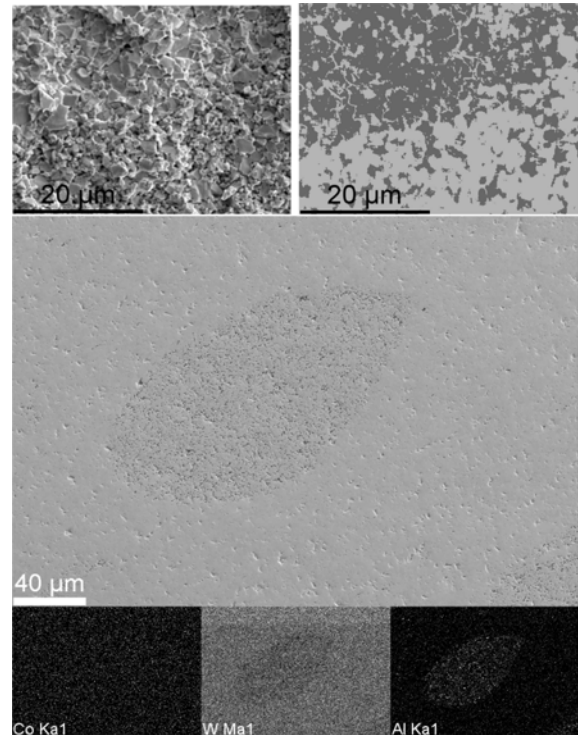


Fig. 5. SEM-EDX of a fracture and polished surface of a compact materials with ALD treatment after sintering. (a) fractured cross-section of sintered WC-8Co with 70 ALD cycles, (b) element map: W is corresponding to dark grey, Al is corresponding to light grey, (c) polished cross-section of sintered WC-8Co with 150 ALD cycles and elemental map.

Average crystallite sizes of tungsten carbide obtained from Rietveld refinement of XRD data were 68 nm for WC-8Co powder, 129 nm for sintered sample treated during 150 ALD cycles, 222 nm for sintered sample treated during 70 ALD cycles, and 198 nm for sintered sample without ALD treatment. The lowest average crystallite size of the sintered WC-8Co is referring to the samples with the thicker alumina coating.

The presence of aluminum oxide on the tungsten carbide grain boundaries can be seen at fracture and polished sections (Fig. 5). At SEM images of the polished section can be seen porous areas around 20-100 μm enriched by aluminum oxide. The local areas with high alumina content could be related with sintering of agglomerates with the alumina coating thicker than 100 nm. The sintering of alumina can be difficult because of its rhombohedral lattice structure where all three parameters are different and the adhesion between Al_2O_3 coatings is poor. It may be the reason of porosity formation in places with high content of aluminum oxide. Low surface porosity at the polished sample may be associated with spalling of WC particles in consequence of which could stay locations with recesses.

Macro-hardness values of spark plasma sintered samples were 1861.42 ± 31.73 MPa for sample treated during 150 ALD cycles, 1855.17 ± 58.37 MPa for compact cemented carbide treated during 70 ALD cycles, 1752.48

± 58.29 for sintered cemented carbide without ALD treatment. Macro hardness slightly increase with alumina addition.

The density of the sintered samples with and without of aluminum oxide films measured by hydrostatic weighing is about 99.0-99.6% of the theoretical value.

Conclusions

This study examines the process of aluminum oxide films deposition on the WC-8Co cemented carbide powder by atomic layer deposition. The coatings of alumina were found both on separate particles and dense agglomerates. Fewer ALD cycles produce thinner coatings. The thickness of aluminum oxide was higher after 150 ALD cycles. The thickness ranges from 30 to 100 nm depending on the density of powder filling.

The compact nanocomposites were made using spark plasma sintering (SPS). According to XRD data, sintered samples consist only of the WC phase. According to [11], the addition of small amount of aluminum oxide prevents the formation of W_2C during sintering. In addition, the SPS method decreases the W_2C phase content in the sintered samples. The lowest average crystallite size about 129 nm of the sintered WC-8Co refers to the samples with thicker alumina coating. The chemical composition of fracture shows the presence of aluminum oxide at the grain boundaries of tungsten carbide. The polished samples displayed porous areas enriched by aluminum oxide. The local areas with high alumina content can be related with sintering of agglomerates with thick alumina coating. The macro hardness slightly increases with alumina addition. The density of the sintered samples with and without aluminum oxide was about 99-99.6% of the theoretical value.

References

1. V.S. Panov, A.M. Chuvilin, and V.A. Falkowskii, in "Technology and properties of sintered hard alloys and products from them", Moscow Institute of Steel and Alloys (2004).
2. V. Sarin, in "Comprehensive hard materials Vol. 2", Elsevier (2014) 50.
3. V.F. Mazanko, A.V. Pokoyev, V.M. Mironov, D.S. Gertsriken, D.V. Mironov, D.I. Stepanov, and G.V. Lutsenko, in "Diffusion in metals under magnetic fields and high speed deformation Vol. 1", Mashinostroyeniye (2005) 253.
4. S.I. Cha, S.H. Hong, and B.K. Kim, Mater. Sci. Eng. A 351[1] (2003) 31-38.
5. C.C. Jia, H. Tang, X.Z. Mei, F.Z. Yin, and X.H. Qu, Mater. Lett. 59[19] (2005) 2566-2569.
6. D. Sivaprahasam, S.B. Chandrasekar, and R. Sundaresan, Int. J. Refract. Met. Hard Mater. 25[2] (2007) 144.
7. S.V. Nikolenko, A.D. Verhoturov, M.I. Dvornik, N.M. Vlasova, M.A. Pugachevsky, M.M. Mihailov, and N.S. Krestjanikova, Problems of Materials Science 54[2] (2008) 100-106.
8. A.M. Salakhov, in "Vvedeniye v tekhnologiyu konstruktsionnykh materialov [Introduction to the technology of construction materials]" (Kazan Federal University, 2014) p. 68.
9. J.M. Keane, Wire J. Int. 45[8] (2012) 72-77.
10. R.E. Toth, I. Smid, J. Keane, R.M. German, and P. Ettmayer, in 2004 European PM Conf. Proc. (Vienna) Vol. 3 (Shrewsbury: European Powder Metallurgy Association (EPMA)) p. 1.
11. D. Zheng, X. Li, X. Ai, C. Yang, and Y. Li, Int. J. Refract. Met. Hard Mater. 30[1] (2012) 51-56.
12. E.M. Pallone, D.R. Martin, R. Tomasi, and W.J. Botta Filho, Mater. Sci. Eng. A 464[1] (2007) 47-51.
13. W.P. Tai and T. Watanabe, J. Am. Ceram. Soc. 81[6] (1998) 1673-1676.
14. S.M. George, Chem. Rev. 110[1] (2010) 111-131.
15. M. Leskelä and M. Ritala, Angew. Chem. Int. Ed. 42[45] (2003) 5548-5554.
16. V. Miikkulainen, M. Leskelä, M. Ritala, and R.L. Puurunen, J. Appl. Phys. 113[2] (2013) 021301.